Cheung, K. K. W., Ozturk, U. (2020): Synchronization of extreme rainfall during the Australian summer monsoon: Complex network perspectives. - Chaos, 30, 063117.

https://doi.org/10.1063/1.5144150

Synchronization of extreme rainfall during the Australian summer monsoon: Complex network perspectives

Cite as: Chaos **30**, 063117 (2020); https://doi.org/10.1063/1.5144150
Submitted: 03 January 2020 . Accepted: 08 May 2020 . Published Online: 04 June 2020

Kevin K. W. Cheung, and Ugur Ozturk

Synchronization of extreme rainfall during the Australian summer monsoon: Complex network perspectives

Cite as: Chaos **30**, 063117 (2020); doi: 10.1063/1.5144150
Submitted: 3 January 2020 · Accepted: 8 May 2020 ·
Published Online: 4 June 2020

Kevin K. W. Cheung[1,a)] and Ugur Ozturk[2]

AFFILIATIONS

[1]Department of Earth and Environmental Sciences, Macquarie University, North Ryde, NSW 2109, Australia
[2]Helmholtz-Zentrum Potsdam, Deutsches GeoForschungsZentrum GFZ, Telegrafenberg, 14473 Potsdam, Germany

Note: This article is part of the Focus Issue, Rare Events in Complex Systems: Understanding and Prediciton.
[a)]**Author to whom correspondence should be addressed:** kevin.cheung@mq.edu.au

ABSTRACT

Monsoon rains are an important fresh water supply for agricultural activity, while extreme rainfalls during a monsoon season frequently cause flash floods. In this study, a nonlinear causation measure of event synchronization is used to set complex networks of extreme rainfall during the Australian summer monsoon (ASM) development between 1st November and 1st March. We adopted Tropical Rainfall Measuring Mission-based satellite rain rate estimates from 1998 to 2015. Examining several standard network centrality measures, such as degree and local clustering, we revealed the multiscale nature of ASM development, which previously was only studied by weather analysis methods. The land–sea contrast in surface heating critical for ASM is depicted clearly by the degree centrality. In addition, both the clustering coefficient and the community structure show critical change in spatial pattern matching with the climatological average onset time of the ASM during late December. The former is likely related to the interaction between synoptic forcing and mesoscale convection during monsoon onset, resulting in characteristic changes in the rainfall field. One of the network communities also extends spatially during the onset, revealing critical information from the near-equatorial region to ASM and would be applicable to monitor monsoon development. Results from this study further support that network measures as defined by a single parameter of rainfall have enormous potential for monsoon onset prediction.

Extreme rainfall from monsoons provides critical sources of fresh water but at the same time presents a potential threat of flooding to the regions involved. Complex network is an emerging method to identify the temporal and spatial patterns of extreme rainfall and potentially also to reveal the underlying dynamics of the associated weather processes. We use a measure of synchronization of extreme rainfall events to define networks during the Australian summer monsoon development. Various network centrality metrics, such as degree and clustering coefficient, are able to reveal the multiscale nature of the monsoon as well as the critical factors such as land–sea contrast through the spatial characteristics of rainfall. The results provide ample potential for monsoon onset prediction based on network metrics and with minimal input parameters.

I. INTRODUCTION

Extreme rainfall is often associated with monsoons and severe weather systems, such as fronts, tropical and local storms, and mesoscale convective systems[1] (MCSs). Those extreme rainfall events often lead to meteorological hazards that cause economic losses and even human casualties. Improving the understanding of their physical mechanisms and representation in numerical models has been the long-term goal of atmospheric scientists and those performing climate projection. These extreme rainfall events possess a time scale from hours, days, to a season, thus resulting in a wide range of predictability issues, and the moist processes generating rainfall remain one of the most uncertain aspects in climate projection.

Being one of the major monsoon regions, the Australian summer monsoon (ASM) develops during late December and early

January south of the equator over longitudes across the Australian continent and western South Pacific, although the exact domain is debatable.[2] It is not an isolated system due to well-known interactions with the East Asian monsoon system on a biennial time scale.[3] The ASM is one of the major sources of fresh water for northern Australia; however, torrential rainfall from it also results in extensive flood events. Similar to other monsoon systems in the Northern Hemisphere, the ASM develops with its onset phase, with multiple burst periods of extreme rainfall in the season and relatively dry period in between. The synoptic factors responsible for the onset of ASM and convection pattern including the MCS activities in a season have been quite well studied in the past (Fig. 1).[4–6]

Extreme rainfall events also possess a wide range of spatial scales, and the types of forcing behind, e.g., frontal systems are largely due to synoptic forcing. On the other hand, for rainbands in tropical storms and mesoscale systems such as MCS, the storm dynamics determine the rain pattern. The monsoons are another example of possessing multiscale forcing during their development.[7,8] Synoptic factors including land–sea contrast are essential and at the same time MCSs embedded in monsoon circulation generate some of the most extreme precipitation.[8] When a precipitation system of certain size develops, rainfall at locations within the system is expected to possess certain degree of synchronization.[9] If this concept is applied in the reversed sense, namely, analysis of the degree of synchronization of rainfall with respect to spatial locations will be able to reveal the scales of the underlying physical processes generating the extreme rainfall.[10,11] This study adopts this approach with the application of a complex network.

The concept of the complex network is an emerging method to analyze extreme rainfall during monsoon development and has been applied to several major monsoon regions.[12] For example, the synoptic factors, topography, moisture sources and sinks, and decadal variability of the South Asian[13] or Indian summer monsoon have been revealed by complex network analysis.[14,15] Within a season of the Indian monsoon, network structures can also show distinct features during the pre-monsoon and post-monsoon periods.[16] Similarly, moisture pathways and contribution from MCSs during the South American monsoon was identified based on synchronicity and the complex network.[17] Complex network has also been applied to study rainfall from weather systems such as the Baiu/Meiyu front and tropical cyclones and able to identify the distinct characteristics from these two systems.[18,19]

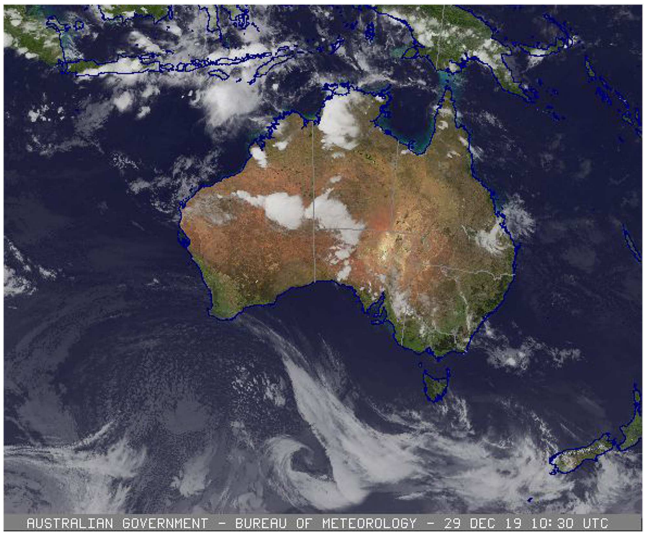

FIG. 1. Infrared satellite image showing the organized cloud clusters to the north of Australia and those over the continent at 10:30 UTC 29 December 2019 (Satellite image originally processed by the Australian Bureau of Meteorology from the geostationary satellite Himawari-8 operated by the Japan Meteorological Agency. Blue Marble surface image courtesy of NASA).

II. DATA AND METHODOLOGY

A. Satellite rainfall data

In this study, data from the NASA/JAXA Tropical Rainfall Measuring Mission (TRMM) multi-satellite precipitation analysis (TMPA) is utilized.[20] The L3-3B42 (V7) gridded dataset is provided three-hourly or daily with 0.25° resolution in both latitude and longitude. The entire period of availability of TRMM 3B42 (1998–2015) is applied to avoid potential issues from transition to the new satellite and analysis scheme after 2015.[21]

We used the daily TRMM-3B42 (V7) data in our analyses instead of the primary three-hourly product. The resulted network would be determined by the highly stochastic convective bursts, and the synoptic and mesoscale processes cannot be clearly revealed, if synchronization of rainfall events is separated as short as 3 h. The study period is the Austral summer season from November to the next March covering the entire ASM, roughly around late December to early February.

B. Event synchronization

In early studies of the climate network, often the link in a network is defined based on the linear correlation coefficient.[22–25] In this study, the nonlinear correlation measure of event synchronization (ES) for a time series with well-defined events[9,14,26] is applied, which is better suited for event based time series as rainfall.

We define extreme rainfall events in each time series based on a peak-over-threshold method that sets all events above the ρ^{th} percentile as extremes in each time series.[14,15,18,19,26] Given that more severe rainfall would occur during monsoon development, such percentile method to define the extremes should be more appropriate than a fixed threshold method. There are also many other popular and accepted extreme indices for precipitation in the literature, such as the maximum precipitation within a certain period (e.g., 1 day or 5 days), as recommended by the Commission for Climatology (CCI)/Climate Variability and Predictability (CLIVAR)/Joint Technical Commission for Oceanography and Marine Meteorology (JCOMM) Expert Team on Climate Change Detection and Indices (ETCCDI).[27] However, it is our purpose of identifying the extremes out of the intermittent rainfall time series without imposing a fixed period for identification. As such, the ES method with a percentile as threshold well fits into our purpose.

To measure the degree of ES between two event time series, we first compute time t^i_l at which an event l occurs at grid i, $l = 1, 2,$

$3, \ldots, s_i$, where s_i is the total number of extreme events in the time series that occur over grid i. This event l is considered to be synchronized with another event m that occurred at t^j_m in the grid j ($m = 1, 2, 3, \ldots, s_j$), when they occur within a time interval T^{ij}_{lm},

$$T^{ij}_{lm} = \frac{min\{t^i_l - t^i_{l-1}, t^i_{l+1} - t^i_l, t^j_m - t^j_{m-1}, t^j_{m+1} - t^j_m\}}{2}, \quad (1)$$

where T^{ij}_{lm} is the shortest interval between the preceding and the successive events, and it is adaptive, i.e., it varies with changing frequency of events.[14,15,18,19] Next, we calculate $c(i|j)$, the number of synchronized events at grid i with grid j and vice versa $c(j|i)$,

$$c(i|j) = \sum_{l=1}^{s_i} \sum_{m=1}^{s_j} J^{lm}_{ij} \quad (2)$$

for all pairs of events within the time interval of T^{ij}_{lm} using a weight J^{lm}_{ij} to avoid counting the paired events two times when the paired events are counted at grid j with grid I,[14,15,18,19]

$$J^{lm}_{ij} = \begin{cases} 1 & if\ 0 < t^i_l - t^j_m \\ \frac{1}{2} & if\ t^i_l - t^j_m = 0 \\ 0 & \text{else} \end{cases}. \quad (3)$$

That is, if the synchronized events l and m occur in the same time $t^i_l = t^j_m$, then $J^{lm}_{ij} = 0.5$, so as $J^{ml}_{ji} = 0.5$; if the event first happens at grid i in j($t^i_l < t^j_m$), then $J^{lm}_{ij} = 1$, whereas $J^{lm}_{ij} = 0$.[14,15,18,19]

Then, the strength of ES between the grid i and j is given by

$$Q_{ij} = \frac{c(i|j) + c(j|i)}{\sqrt{(s_i - 2) \cdot (s_j - 2)}}. \quad (4)$$

Q_{ij} is a symmetric quantity, i.e., $Q_{ij} = Q_{ji}$ and where $0 \le Q_{ij} \le 1$, $Q_{ij} = 1$ implies complete synchronization between grid i and j.[25]

For our analysis, we calculate a Q_{ij} matrix for the TRMM data, which consists of daily rainfall recorded over a spatial grid, extending from −20.125°S to −4.875°S latitudinally and 99.875°E to 160.125°E longitudinally. Each cell within the spatial grid has a spatial resolution of 0.25°, i.e., we have 15 004 grid cells covering the whole study region. Hence, the dimensions of the Q_{ij} matrix are 15 004 × 15 004. We refer to the ES matrix calculated using the ρth percentile threshold for defining an extreme event as Q^ρ_{ij}.

To construct a network from the Q^ρ_{ij} matrix, we treat the spatial grid points of the TRMM data as nodes of a network and edges between these nodes exist only if Q^ρ_{ij} is above a certain threshold. As the largest values in Q^ρ_{ij} are the outcomes of the most correlated atmospheric features, we assume grids (nodes) above the 95th percentile (named γ) of Q^ρ_{ij} values are connected. In other words, the edges (links) are between nodes with the top 5% of the Q^ρ_{ij} values. An undirected network is represented by a binary square matrix, known as the adjacency matrix $A^{\rho\gamma}_{ij}$ (equals to 0 for $i = j$), obtaining as follows:

$$A^{\rho\gamma}_{ij} = \begin{cases} 1 & \text{if } Q^\rho_{ij} \ge \alpha(\gamma) \\ 0 & \text{if } Q^\rho_{ij} < \alpha(\gamma) \end{cases}, \quad (5)$$

where $\alpha(\gamma)$ is the corresponding threshold on Q^ρ_{ij} for a given γ. If there exists an edge between grid i and j, then $A^{\rho\gamma}_{ij} = 1$, else $A^{\rho\gamma}_{ij} = 0$.

To apply ES to the development of ASM, a rainfall time series window of 60 days (i.e., nearly 2 months) each year from TRMM is selected. Since there are a total of 18 years of TRMM data, a time series has 1080 data points. Extreme rainfall is defined as daily rain equal to or higher than the 90th (i.e., ρth) percentile in the time series, leading to 108 extreme events for the ES algorithm. The first 60-day period begins from 1st November, and we shift this period every 5 days until the last one ending on 1st March. By examining the ES-based network measures from these shifting periods, we analyze the climatological development of the ASM.

III. NETWORK MEASURES

A. Definitions

We adopted commonly used network centrality metrics to study the ASM development. First, we use the degree centrality k that counts the number of connections of a node in a network. The k of the node i is

$$k_i = \sum_{j=1}^{n} A_{ij}, \quad (6)$$

where n is the total number of nodes in a network, and A_{ij} indexes whether there is an edge between nodes i and j. Degree centrality gives a quick overview of the collective behavior of network nodes during a rainfall event. Highly connected regions will have large k values, where these regions are the ones where rainfall is an outcome of large-scale spatial atmospheric processes.[14] Before extreme incidents, the connectivity between different regions might change.[28]

We also use clustering coefficient C, which quantifies the geographically clustered connected nodes, to identify collective rainfall behavior in different regions.[19,29] Mathematically, it measures the frequency of triangles in a network, i.e., the number of three-vertex cliques (triangles) in which all three nodes are connected. The C of the node i,

$$C_i = \frac{\sum_{j,h} A_{ij} A_{ih} A_{jh}}{k_i(k_i - 1)} \quad (7)$$

sums over all nearest neighbors j and h of node i, and where A_{ij}, A_{ih}, and A_{jh} indicate whether there is an edge between node i and j, i and h, j and h, respectively, and k_i is the degree. This definition is equivalent to the ratio of the number of links among the neighbors of node i to the total possible number of links among the neighbors. The local clustering coefficient measures the ratio of links connecting the direct neighbors of a particular node to the number of all possible links between them,[30] and it is a characteristic of the spatial continuity of the rainfall field.

We lastly study communities that best partition our networks based on maximizing modularity of the network.[31,32] Communities in a network represent groups of nodes that are highly connected within each community but with weaker links among the communities.[33] These communities are representative of coherent rainfall zones over the study area, i.e., the rainfall over these zones is more homogeneous, synchronized, and have similar dynamical properties.

B. Evolution during ASM development

The first network measure to examine is the degree centrality, which reveals the connectivity within the rainfall network. Throughout the shifting periods from November to March, the spatial pattern of the degree does not vary much. The most distinct feature of the degree is the contrast between the land and sea locations, with the highest degree (about ∼5000 that is about one-third of the total number of grid points) over the land including the northern Australia and the Indonesia and Papua New Guinea (PNG) (Fig. 1). Comparatively, the degree over the ocean is much lower. This is believed to be related to convection forced by land heating that drives more synchronized rainfall events.

While the spatial pattern of the degree does not change much during the entire period of analysis, for 60-day periods after the onset of ASM, the maximum degree has decreased to about 4000 [Fig. 1(b)] and this persists for all the later analysis periods.

Such overall reduction in the degree can also be depicted in the evolution of the link distribution within the network. When our analysis period starts from early October and progresses to December, it can be seen that the mean link distance has shifted to the smaller side (Fig. 2). Initially the change in link distribution is small; however, for periods starting late November and early December, the change accelerates.

The clustering coefficient, on the other hand, possesses higher values over the ocean surface, including that north and northeast of the Australian continent (Fig. 3). In contrast, the clustering coefficient over the tropical Australian land has almost the lowest values in the domain of analysis. Such contrast indicates that the rainfall pattern over the tropical oceans is smoother than that over land, which may be due to the forcing from the slowly varying and warm sea surface temperature during the Austral summer. Note that the largest cluster with highest clustering coefficient values is at the South Indian Ocean (northwest of Australia).

Unlike the degree, the cluster coefficient has interesting evolution during the ASM development. For periods centering before mid-December, the values are high over all ocean surfaces [an example in Fig. 3(a)]. However, after the average onset date of 25 December,[4] the coefficient value decreases substantially over the regions north of Australia [an example in Fig. 3(b)]. This is closely related to the synoptic factors leading to the ASM onset and the associated responses in the rainfall pattern, as will be discussed in Sec. IV.

Community analysis is able to reveal the collective behavior within groups of nodes of the complex network, and in our case synchronized rainfall during ASM development. For all the periods of analysis, seven communities have been identified (Fig. 4). One major community is at the tropical ocean north of Australia (number 1 in the figure), and the other six communities surrounding the central one.

The spatial pattern of the seven communities does not change much during the ASM development. One distinct feature is that near the average onset date of late-December, the community over the Indonesian region (number 2 in Fig. 4) has been expanding to the west and also crossing over to the east and eventually covers

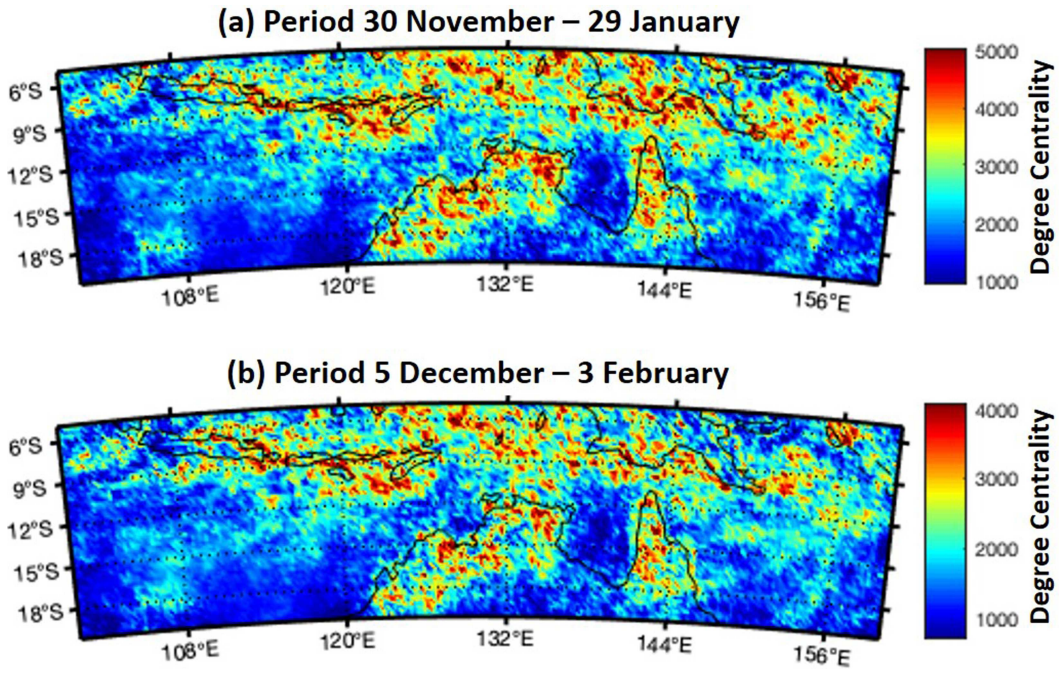

FIG. 2. Degree centrality for the analysis period: (a) 30 November–29 January and (b) 5 December–3 February.

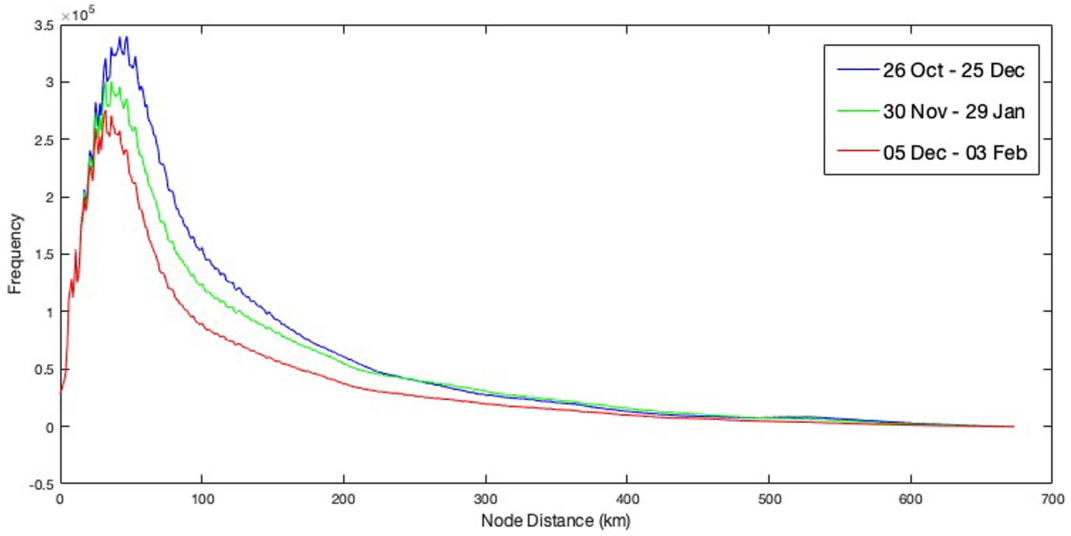

FIG. 3. Link-length distributions in the rainfall network for the period 26 October–25 December (blue), 30 November–29 January (green), and 5 December–3 February (red). The distributions have been smoothed using running means over 5 bins, i.e., 15 km.

part of the PNG. This large community then persists after the ASM onset.

Note that the community 1 north of Australia actually coincides with the region with the most substantial change in the clustering coefficient during ASM development, which depicts changes in the convective and mesoscale rainfall in that community, while still coherently connected. On the other hand, the expanding community to the north (number 2) is one of the regions with high degree in Fig. 1. The expansion of this community indicates that synoptic factors have led to synchronized extreme rainfall events over a larger area during the onset of ASM, and there is transfer of the influence of these synoptic factors to both the east and west.

It should be noted that finite domain analysis would have effect on the estimates of the network measures especially for those near the domain boundary. Due to limitation of computer time, the measures shown in Figs. 2, 4, and 5 have not been boundary corrected. However, such correction would not change our major conclusions as the spatial patterns of these measures remain the same qualitatively.

IV. METEOROLOGICAL INTERPRETATION

The ASM is well-known to be multiscale in nature during its development. During the Boreal winter, the intertropical convergence zone (ITCZ) over the western Pacific shifts to the southern hemisphere, leading to moisture convergence to the north of Australia.[34] Associated with this shift of the ITCZ, the ASM is often defined as the establishment of wet westerlies in the tropical Australian region.[4] The average onset date is 25 December; however, standard deviation is as large as 16 days.

Hung and Yanai[5] summarized the synoptic factors pacing for the onset of ASM. These include the land–sea contrast, barotropic instability for convection development, midlatitude trough influence, and effect from the Madden-Julian 40–50-day Oscillation (MJO) that has also been identified in Hendon and Liebmann.[4] The land–sea contrast is a fundamental setup of monsoon development. For the ASM, surface heat low would develop over land and the associated low-level convergence, together with the meridional temperature gradient, would draw in moisture from the tropics to northern Australia that lead to severe convection development.

The used network metrics have revealed the multiscale nature of ASM nicely. First, the land–sea contrast has been identified in the degree centrality (Fig. 1), with the largest degree over land. This is due to the larger surface heating from land that leads to convection and rainfall in more synchronized way.

However, during the onset of ASM, one of the major features is organized convection to the north of Australia, and it is exactly in such organized convection there is strong interplay between the mesoscale and synoptic processes. There are several synoptic factors responsible for organizing the convection, which include midlatitude trough[5] and upper-level anticyclone.[4,35] Keenan and Brody[35] identified the major bands of organized convection via infrared satellite images and found that most of them were within the latitudinal band 10°–15°S and some just south of the equator (see their Fig. 5, also Ref. 36). Within these organized convection band, May[8] also identified abundant MCSs embedded inside, and a lot of convective centers were accompanied by stratiform rain regions.

Such organized convection concentrates north of the Australian continent that coincides with the regions with the highest clustering coefficient (Fig. 3). Since the clustering coefficient is a measure of smoothness in the network, the large values identified are likely due to the highly synchronized rainfall within the convection bands. After the monsoon onset, there are multiple, alternating

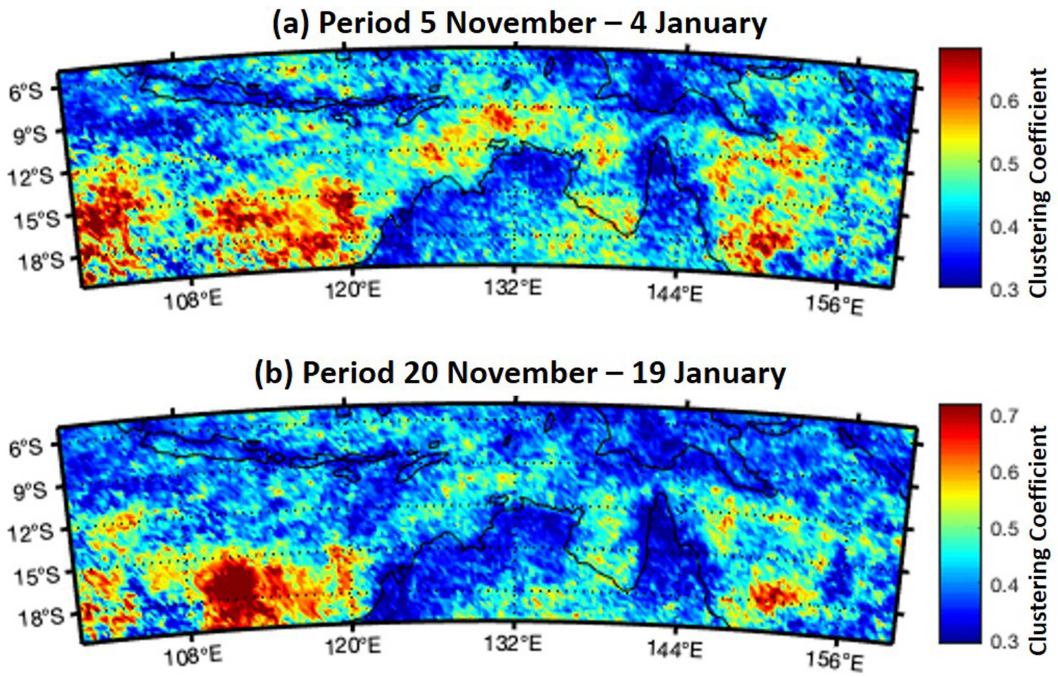

FIG. 4. Clustering coefficient for the analysis period: (a) 5 November–4 January and (b) 20 November–19 January.

periods of active (with convective bursts) and inactive (relatively dry) rainfall.[37] Thus, when our sliding analysis periods are after the average onset time, the clustering coefficient decreases substantially when there are less persistent organized cloud clusters.

On a separate note, Fig. 3 also shows a region with large clustering coefficient values within 100°–120°E northwest of Australia, which indicates organized convection. This is likely due to the disturbances originated from the South Indian Ocean.[38] Wave trains from that Ocean may travel north-eastward, thus enhancing the monsoon trough development.[6]

The identified network communities are also consistent with our understanding of the synoptic factors for establishing the ASM. The central community north of the Australian continent in Fig. 4 is the critical region where the monsoon trough develops during the monsoon onset (mentioned in Sec. III B). Moreover, the community to the north first concentrates in the Indonesian region with the organized convection over there. Then this community extends to the east, indicating that during the ASM onset, organized convection and associated synchronized extreme rainfall would extend to the PNG region. Such extension of the coherent rainfall pattern may be a critical factor to monitor the ASM development.

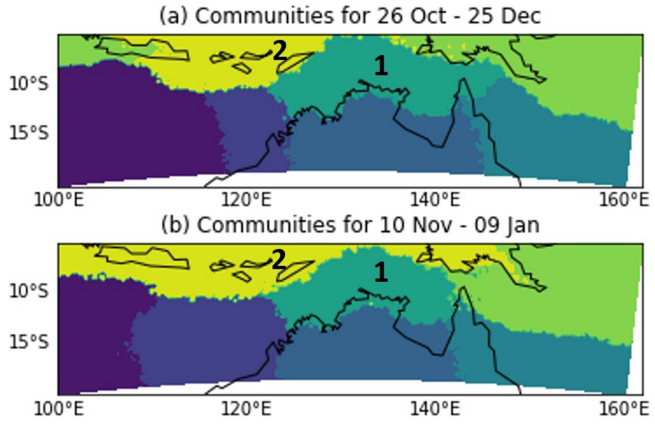

FIG. 5. The seven communities identified for period (a) 26 October–25 December and (b) 10 November–9 January. Numbers 1 and 2 have been marked.

V. SUMMARY

In summary, this is the first study to apply the common nonlinear measure of event synchronization to define the complex network of extreme rainfall during the Australian summer monsoon development. The TRMM-3B42 daily rainfall is used to identify the extreme rain events above the 90th percentile. Five daily sliding time windows with a 60-day period from November to March are analyzed to monitor the changes in network metrics during the climatological onset date of the ASM in late December.

Some of the fundamental factors and the multiscale nature of the ASM development, which are identified previously through traditional weather analysis, are revealed by the network metrics. The land–sea contrast in surface heating would generate different cloud and rain characteristics and has been depicted clearly by the spatial

pattern of the degree centrality. The rainfall network generally has higher degree over land.

In addition, both the clustering coefficient and the community structure show a critical change in their spatial pattern matching with the climatological average onset time of the ASM during late December. The clustering coefficient is high in the region where the monsoon trough is strengthening before the ASM onset, which is likely related to the organized convection due to the interaction between synoptic forcing and mesoscale convection during the onset, resulting in characteristic changes in the rainfall field. Such multiscale nature of the ASM has been extensively studied in the literature.

One of the network communities coincides with the monsoon trough region north of Australia. Another community further to the north extends spatially during the monsoon onset, indicating that the region of coherent and highly synchronized rainfall pattern first resides over the Indonesian region and then extends to the east during the setup of monsoon. This reveals that processes in the near-equatorial region are critical to ASM development.

Different from the traditional weather analysis of atmospheric processes, our network study has diagnosed many key features of the ASM onset through only the analysis of synchronized extreme rainfall events. This further supports the notion that precipitation as the outcome of the atmospheric/oceanic processes is a critical parameter to analyze and in accord with the concept of global monsoon.[2] That is, the monsoon systems should be defined as the modes of tropical rainfall variability instead of only through seasonal wind reversal. Our application of complex network has opened up a new paradigm of methodology along this research direction.

Besides merely being used for diagnostic purposes, the complex network applied to monsoon studies has demonstrated its potential for prediction when certain network metrics are able to indicate critical physical mechanisms responsible for the extreme rainfall events.[28] In our case of ASM, it is quite clear that the clustering coefficient and network community are good candidates to develop a prediction model for the ASM onset. The first thing that needs refinement would be to extend our analysis to examine the interannual variability of the ASM and how the rainfall network correlates.[15]

The network analysis results presented here are at the preliminary stage and future work is going to provide an understanding of the wind systems in the ASM region and how they are linked to the network structure.[16] At the more fundamental level, the multiscale nature and interaction between synoptic and mesoscale processes should be studied more in-depth through examination of the evolution of specific rainfall fields in association with the network metrics.

ACKNOWLEDGMENTS

Ugur Ozturk is funded by the Federal Ministry of Education and Research (BMBF) within the Project CLIENT II-CaTeNA (No. FKZ 03G0878A). The Tropical Rainfall Measuring Mission (TRMM) data were obtained from NASA and the Japan Aerospace Exploration Agency (JAXA). The two anonymous reviewers' comments have greatly improved the manuscript.

DATA AVAILABILITY

The data that support the findings of this study are openly available in the U.S. National Aeronautics and Space Administration (NASA) at http://dx.doi.org/10.5067/TRMM/TMPA/3H/7, Ref. 20.

REFERENCES

[1]R. A. Houze, Jr., "100 years of research on mesoscale convective systems," in *A Century of Progress in Atmospheric and Related Sciences: Celebrating the American Meteorological Society Centennial*, AMS Monograph (2018).
[2]B. Wang and Q. Ding, Dynam. Atmos. Oceans **44**, 165–183 (2008).
[3]C.-P. Chang and T. Li, J. Atmos. Sci. **57**, 2209–2224 (2000).
[4]H. H. Hendon and B. Liebmann, J. Atmos. Sci. **47**, 2227–2240 (1990).
[5]C.-W. Hung and M. Yanai, Q. J. R. Meteorol. Soc. **130**, 739–758 (2004).
[6]N. E. Davidson, K. J. Tory, M. J. Reeder, and W. L. Drosdowsky, J. Atmos. Sci. **64**, 3475–3498 (2007).
[7]B. Mapes *et al.*, "Heaviest precipitation events 1998–2007: A near-global survey," in *The Global Monsoon System: Research and Forecast*, 2nd ed., edited by C.-P. Chang (World Scientific, Singapore, 2011).
[8]P. May *et al.*, "Mesoscale aspects of the Australian monsoon," in *The Global Monsoon System: Research and Forecast*, 2nd ed., edited by C.-P. Chang (World Scientific, Singapore, 2011).
[9]A. Agarwal, N. Marwan, M. Rathinasamy, B. Merz, and J. Kurths, Nonlin. Processes Geophys. **24**, 599–611 (2017).
[10]A. Agarwal, N. Marwan, R. Maheswaran, B. Merz, and J. Kurths, J. Hydrol. **563**, 802–810 (2018).
[11]J. Kurths, A. Agarwal, R. Shukla, N. Marwan, M. Rathinasamy, L. Caesar, R. Krishnan, and B. Merz, Nonlin. Processes Geophys. **26**, 251–266 (2019).
[12]F. Wolf, J. Bauer, N. Boers, and R. V. Donner, Chaos **30**, 033102 (2020).
[13]M. Gelbrecht, N. Boers, and J. Kurths, Sci. Adv. **4**, eaau3191 (2018).
[14]N. Malik, N. Marwan, and J. Kurths, Nonlin. Processes Geophys. **17**, 371–381 (2010).
[15]N. Malik, B. Bookhagen, N. Marwan, and J. Kurths, Clim. Dyn. **39**, 971–987 (2012).
[16]V. Stolbova, P. Martin, B. Bookhagen, N. Marwan, and J. Kurths, Nonlin. Processes. Geophys. **21**, 901–917 (2014).
[17]N. Boers, B. Bookhagen, N. Marwan, J. Kurths, and J. Marengo, Geophys. Res. Lett. **40**, 4386–4392, https://doi.org/10.1002/grl.50681 (2013).
[18]U. Ozturk, N. Marwan, O. Korup, H. Saito, A. Agarwal, M. J. Grossman, M. Zaiki, and J. Kurths, Chaos **28**, 075301 (2018).
[19]U. Ozturk, N. Malik, K. Cheung, N. Marwan, and J. Kurths, Clim. Dyn. **53**, 521–532 (2019).
[20]Tropical Rainfall Measuring Mission (TRMM), "TRMM (TMPA) rainfall estimate L3 3 hour 0.25 degree x 0.25 degree V7," Greenbelt, MD, Goddard Earth Sciences Data and Information Services Center (GES DISC), https://doi.org/10.5067/TRMM/TMPA/3H/7 (Accessed 5 April 2019) (2011).
[21]G. J. Huffman, "The transition in multi-satellite products from TRMM to GPM (TMPA to IMERG)," in *NASA Precipitation Measurement Missions Documentation* (2019), p. 5.
[22]A. A. Tsonis, K. Swanson, and S. Kravtsov, Geophys. Res. Lett. **34**, L13705, https://doi.org/10.1029/2007GL030288 (2007).
[23]K. Yamasaki, A. Gozolchiani, and S. Halvin, Phys. Rev. Lett. **100**, 228501 (2008).
[24]G. Wang, K. L. Swanson, and A. A. Tsonis, Geophys. Res. Lett. **36**, L07708, https://doi.org/10.1029/2009GL036874 (2009).
[25]J. F. Donges, Y. Zou, N. Marwan, and J. Kurths, Eur. Phys. Lett. **87**, 48007 (2009).
[26]R. Q. Quiroga, T. Kreuz, and P. Grassberger, Phys. Rev. E **66**, 04190 (2002).
[27]X. Zhang, L. Alexander, G. C. Hegerl, P. Jones, A. K. Tank, T. C. Peterson, B. Trewin, and F. W. Zwiers, Wiley Interdiscip. Rev. Clim. Change **2**, 851–870 (2011).
[28]N. Boers, B. Bookhagen, H. M. J. Barbosa, N. Marwan, J. Kurths, and J. Marengo, Nat. Commun. **5**, 5199 (2014).
[29]D. J. Watts and S. H. Strogatz, Nature **393**, 440–442 (1998).

[30]S. K. Jha, H. Zhao, F. M. Woldemeskel, and B. Sivakumar, J. Hydrol. **527**, 13–19 (2015).
[31]V. D. Blondel, J.-L. Guillaume, R. Lambiotte, and E. Lefebvre, J. Stat. Mech. **2008**, P10008 (2008).
[32]A. Agarwal, N. Marwan, M. Rathinasamy, U. Ozturk, J. Kurths, and B. Merz, Hydrol. Earth Syst. Sci. Discuss. 24, 2235–2251 (2020).
[33]K. Fang, B. Sivakumar, and F. M. Woldemeskel, J. Hydrol. **545**, 478–493 (2017).
[34]R. Suppiah, Prog. Phys. Geog. **16**, 283–318 (1992).
[35]T. D. Keenan and L. R. Brody, Mon. Weather Rev. **116**, 71–85 (1988).
[36]J. L. McBride, Tellus **35A**, 189–197 (1983).
[37]G. J. Berry and M. J. Reeder, J. Atmos. Sci. **73**, 55–69 (2016).
[38]G. J. Berry, M. J. Reeder, and C. Jakob, J. Clim. **25**, 8409–8421 (2012).